

Efficient Blue-Emitting Ir(III) Complexes with Phenyl-Methyl-Benzimidazolyl and Picolinate Ligands: A DFT and Time-Dependent DFT Study

Ming-Xing Song, Zhao-Min Hao, Zhi-Jian Wu, Shu-Yan Song, Liang Zhou, Rui-Ping Deng, and Hong-Jie Zhang*

The series of heteroleptic cyclometalated Ir(III) complexes for organic light-emitting display application have been investigated theoretically to explore their electronic structures and spectroscopic properties. The geometries, electronic structures, and the lowest-lying singlet absorptions and triplet emissions of Ir-(pmb)₃ and theoretically designed models Ir-(Rpmb)₂pic were investigated with density functional theory (DFT)-based approaches, where pmb = phenyl-methyl-benzimidazolyl, pic = picolinate, and R = H/F. Their structures in the ground and excited states have been optimized at the DFT/B3LYP/LANL2DZ and TDDFT/B3LYP/LANL2DZ levels, and the lowest absorptions

and emissions were evaluated at B3LYP and M062X level of theory, respectively. The mobility of holes and electrons were studied computationally based on the Marcus theory. Calculations of ionization potentials were used to evaluate the injection abilities of holes into these complexes. The reasons for the higher electroluminescence efficiency and phosphorescence quantum yields in Ir-(Rpmb)₂pic than in Ir-(pmb)₃ have been investigated. The designed molecules are expected to be highly emissive in pure-blue region. © 2013 Wiley Periodicals, Inc.

DOI: 10.1002/qua.24379

Introduction

Luminescent transition metal complexes are used in a diverse range of applications, notably as phosphorescent emitters for organic light-emitting displays (OLEDs) and for solid-state lighting.^[1,2] In this regard, cyclometalated iridium(III) complexes have received special attention as dopants for harvesting the otherwise nonemissive triplet states formed in OLEDs.^[3] The complexes are charge neutral and generally have good chemical and photochemical properties, such as high-thermal stability, short lifetime in excited states, and strong spin-orbit coupling effect of heavy metal, which can, to a large extent, partially remove the spin-forbidden nature of the T₁→S₀ radiative relaxation. Among them, iridium (III) complexes are regarded as the most effective materials in OLEDs, because of which, they would display bright phosphorescent emission spanning the whole visible spectra, making them suitable to serve as ideal phosphors for OLED applications.

Among these Ir(III) complexes, green- and red-emitting species have been known for years and successfully fabricated as emitters in OLEDs with high-quantum efficiency.^[4] However, achieving room-temperature blue phosphorescence with high quantum efficiency remains as a challenge, especially for pure-blue.^[5] Generally, useful approaches of the systematic tuning for Ir(III)-based blue emitters are less obvious and have been grouped by Thompson and coworkers:^[6a] (a) use of electron-withdrawing substituents at the cyclometalating ring, for instance, fluoride.^[7] If the fluoride was attached on the main ligand, it can effect the highest occupied molecular orbital (HOMO) level (both from the metal and main ligand orbitals), whereas only slightly affecting the lowest unoccupied molecular orbital (LUMO) level (from the auxiliary ligand); conversely,

if the fluoride was attached on the auxiliary ligand, it can effect the LUMO level more, whereas HOMO level slightly;^[6b] (b) use of ancillary ligands (LL) to tune the HOMO and LUMO energies of Ir complexes, with the emission coming from the metal and the ligands fragments,^[7c,8] this approach based on the electron perturbation of the HOMO–LUMO energy gap; (c) replacement of the heterocyclic fragment of the (C[^]N) ligands, like phenylpyridine, with moieties bearing higher lying LUMO than for the pyridyl ring,^[7a,9] this can raise the energy of both the metal to ligand charge transfer (MLCT) and the ligand centered (LC) transitions. Combined the approaches (b) and (c) above and on the basis of tris (2-phenylpyridine) iridium (III) [Ir(ppy)₃],^[10] which is the best green-emitting material up to now, Sajoto et al. designed and synthesized the blue-emitting material tris (phenyl-methyl-benzimidazolyl) iridium (III) [Ir-(pmb)₃] in 2005, whose emission level is very high in energy, λ_{em}~380 nm, but the quantum yield is quite low (Φ = 0.04).^[6] Conversely, Kawamura et al. demonstrated that the photoluminescence quantum yield of the blue emitter of Iridium (III) bis

M.-X. Song, Z.-M. Hao, Z.-J. Wu, S.-Y. Song, L. Zhou, R.-P. Deng, H.-J. Zhang
State Key Laboratory of Rare Earth Resource Utilization, Changchun Institute of Applied Chemistry, Chinese Academy of Sciences, Changchun 130022, People's Republic of China
E-mail: hongjie@ciac.jl.cn

Contract grant sponsor: National Natural Science Foundation of China; contract grant number: 21071140.

Contract grant sponsor: National Natural Science Foundation of China Major Project; contract grant number: 91122030.

Contract grant sponsor: 863-National High Technology Research and Development Program of China; contract grant number: 2011AA03A407.

Contract grant sponsor: National Natural Science Foundation for Creative Research Group; contract grant number: 20921002.

© 2013 Wiley Periodicals, Inc.

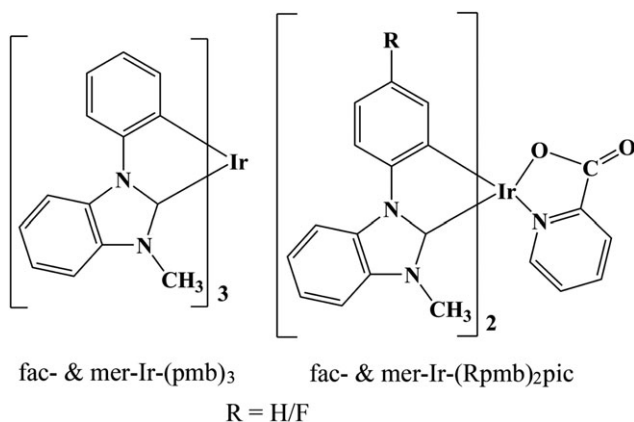


Figure 1. Sketch structures of the complexes.

[(4, 6-difluorophenyl)-pyridinato-N, C²-iridium]picolinate (Firpic) could approach nearly 100% when doped into the wide energy gap (E_g) host of N, N'-dicarbazolyl-3, 5-benzene (mCP) in the same year,^[11] but, it is a standard sky-blue phosphor, λ_{em}~472 nm.^[12] So in here, to find a pure-blue phosphorescent emitting material, we used picolinic acid (pic) as the ancillary ligand to alter the excited-state properties through altering the MLCT energy mainly by changing the LUMO energy level, since the LUMO is mainly localized on the picolinic (pic). We also use the electron-withdrawing substituents fluoride at the cyclometalating ring as the approaches (a) above to adjust the HOMO and LUMO level of the complexes. So we hope to design much more new pure-blue phosphors in OLEDs with high electroluminescence (EL) efficiency and high phosphorescence quantum yields by the methods above.

In contrast to the wide experimental investigations, quantum-chemistry studies on blue-emitting Ir complexes are limited.^[13] To foresee new structure-property relationships and help to improve the design of OLEDs based on blue-emitting iridium(III) complexes, we theoretically investigated the injection, transport, absorption, and phosphorescence properties for a series of blue-emitting iridium(III) complexes facial (fac-) and meridional (mer-) Ir-(Rpmb)₂pic, where R = F/H, using density functional theory (DFT) and time-dependent density-functional theory (TD-DFT). We hope that the study could provide useful information for designing new phosphors in OLEDs with high EL efficiency and high phosphorescence quantum yields.

Methodology

All calculations have been performed with Gaussian09 suite of program with a tight self-consistent field convergence threshold for both gradient and wave function convergence.^[14] The ground-state and the lowest-lying triplet excited-state geometries were optimized by the DFT and the TD-DFT methods with Becke's LYP (B3LYP) exchange–correlation functional, respectively.^[15–17] There were no symmetry constraints on these complexes. The experimental spectral data are obtained in CH₂Cl₂/THF solution, So, at the respective optimized geometries of ground and excited states, TDDFT calculations using the B3LYP functional with the 6-31G (d) and LanL2DZ basis set were used, and the spectral data were associated with the

polarized continuum model (PCM) in medias (absorption in CH₂Cl₂ and emission in THF) with the default parameters embedded in Gaussian09 to obtain a valid approximation of chemical environment,^[18] which have been shown to provide accurate interpretation and prediction for the transition metal complexes in numerous applications in our previous work.^[19] The M062X functional together with the same basis set mentioned above were adopted to evaluate the emission nature.^[20] Furthermore, the stable configurations of these complexes can be confirmed by frequency analysis, in which no imaginary frequency was found for all configurations at the energy minima.

In terms of basis sets, the double-ζ quality 6-31G (d) and LanL2DZ were used for the lighter nonmetallic atoms in ligands (such as C, N, F, and H atoms) and the Ir atom, respectively. A relativistic effective core potential for Ir atom replaces the inner core electrons leaving the outer layer [(5s²) (5p⁶)] electrons and the (5d⁶) valence electrons.^[21] This combination of basis set is adequate to describe the ground and excited state geometries of the Ir (III) complexes, and it has been verified and discussed elsewhere.^[22]

Results and Discussion

Geometries in the ground state S₀ and triplet excited state T₁

The sketch maps of the complexes are shown in Figure 1. The optimized ground-state geometrical structures for the complexes are shown in Figure 2 (Ir-(pmb)₃), Figure S5 (Ir-(pmb)₂pic), and Figure S6 (Ir-(Fpmb)₂pic), along with the numbering of some key atoms. The main geometry structural parameters of the ground states (S₀) of the complexes are summarized in Table 1 together with the X-ray crystal structure data of the Ir-(pmb)₃ complexes [fac- and mer-Ir-(pmb)₃],^[6] from which, we can find that our calculated structural parameters in the Ir-(pmb)₃ complexes are in good agreement with the experimental values, so, the calculation methods we used are feasible. The calculated vibrational frequencies with no imaginary frequency based on the optimized geometries for all the complexes verify that each of the optimized structure is a true minimum on the potential energy surface.

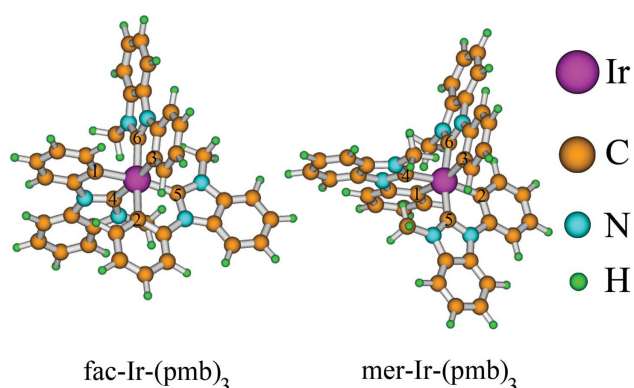


Figure 2. Optimized structures of complexes Ir-(pmb)₃ in the ground states at DFT/B3LYP/LANL2DZ level. [Color figure can be viewed in the online issue, which is available at wileyonlinelibrary.com.]

Table 1. Main optimized geometry structural parameters of the complexes in the ground and the lowest lying triplet states at the B3LYP and CIS level, respectively, together with the experimental values of Ir(pmb)₃ complexes.

Bond	Ir-(pmb) ₃				Ir-(pmb) ₂ pic			Ir-(Fpmb) ₂ pic					
	Facial		Meridional		Facial			Meridional		Facial		Meridional	
	S ₀ (Compl/Exptl ^[a])	T ₁	S ₀ (Compl/Exptl ^[a])	T ₁	S ₀	T ₁	S ₀	T ₁	S ₀	T ₁	S ₀	T ₁	
Selected bond distances (Å)													
Ir—C1	2.108/2.077	2.106	2.127/2.099	2.142									
Ir—C2	2.107/2.071	2.055	2.108/2.078	2.061	2.087	2.040	2.042	2.039	2.083	2.045	2.039	2.039	
Ir—C3	2.108/2.094	2.095	2.121/2.086	2.075	2.043	2.088	2.047	2.018	2.040	2.084	2.045	2.039	
Ir—C4	2.060/2.035	2.094	2.031/2.043	2.173									
Ir—C5	2.063/2.022	2.104	2.016/2.019	2.029	1.988	2.005	2.008	2.000	1.990	2.009	2.009	2.002	
Ir—C6	2.061/2.022	2.071	2.021/2.032	2.015	2.072	2.120	2.028	2.038	2.072	2.118	2.031	2.045	
Ir—O1					2.192	2.041	2.196	2.078	2.184	2.035	2.190	2.067	
Ir—N1					2.155	2.139	2.198	2.213	2.156	2.136	2.194	2.208	
Bond angles (deg)													
1—Ir—C2	92.9/91.0	95.4	96.1/90.9	94.4									
C4—Ir—C6	102.6/100.2	99.3	95.6/94.0	93.6									
C5—Ir—C6	102.6	101.3	168.0	176.6	102.2	103.2	172.2	177.3	101.8	103.3	172.1	176.6	
C2—Ir—C3	93.2	92.3	93.9	109.5	96.7	91.2	90.9	95.1	96.6	91.0	90.9	94.2	
N1—Ir—C2					95.9	96.3	97.7	88.6	90.6	93.3	97.8	88.6	
O1—Ir—C6					95.2	93.9	94.1	85.8	95.4	93.5	94.2	85.6	

[a] Ref. [6].

All complexes maintain the quasi-octahedral geometry around the metal centers as being observed in other typical six-coordinated Ir(III) complexes. But, it should be noted that there are subtle distortion among the structural parameters of them. For fac-isomers, first, Ir-(pmb)₂pic, which is derived from that one of three ligands of Ir-(pmb)₃ was replaced by picolinic acid (pic), the absence of the benzimidazole group in the phenyl-methyl-benzimidazolyl (pmb) ligand reduces the steric hindrance between the pmb ligands and the pic ligand greatly while the interaction between the methyl on benzimidazole group and pic ligand also be reduced. Therefore, the coordination interaction between Ir and N atoms would be stronger in Ir-(pmb)₂pic compared with that in Ir-(pmb)₃ while bond length Ir—N6 is exactly the opposite. Second, to upgrade the LUMO level of Ir-(pmb)₂pic complex, we used fluoride, which is an electron-withdrawing substituent to substitute hydrogen atom at the cyclometalating ring, as shown in Figure 1. So, the bond length Ir—C2, Ir—C3, and Ir—O get longer in complex Ir-(Fpmb)₂pic than they were in Ir-(pmb)₂pic. For the mer-isomers, the twist is larger, and the same reasoning can be used to explain it. The slight elongation of the calculated metal-ligand distances compared with the experimental values can be attributed to the crystal packing in the crystalline state.

It is interesting that the Ir—C6 bond lengths are longer than the Ir—C5 ones in fac-Ir-(Rpmb)₂pic complexes. Generally, for fac-Ir-(pmb)₃ complex, the Ir—C6 and Ir—C5 bond lengths suggest a nearly identical coordination environment around the Ir center, thus, both of them are very similar. But the π -electron delocalization of the pic ligand, which is used in fac-Ir-(Rpmb)₂pic complexes, is smaller than that of (F)pmb ligand. When we used ancillary ligand pic in the complexes, the cooperative effect between the metal and ancillary ligand was decreased; conversely, the ligand pic has a poorer steric hindrance, which makes the coordination interaction smaller

between ligand pic and (F)pmb. Thus, for fac-Ir-(Rpmb)₂pic complexes, the bond lengths Ir—C getting smaller except for Ir—C6 compare to the fac-Ir-(pmb)₃ complex. This is also reflected in the Ir—C2 and Ir—C3 bond lengths, in which the Ir—C2 bond length is longer than the Ir—C3 bond length. Similarly, the steric repulsion between adjacent hydrogen atoms on the phenyl and benzimidazolyl moieties also make the meridional isomers twisted.

The calculated geometrical parameters of the lowest-lying triplet excited states (T₁) of the complexes are also listed in Table 1. The complexes Ir-(pmb)₃ show a slight changes in structure between the singlet ground state and the triplet excited state, and for the other isomers, however, bond lengths Ir—O1 are contracted seriously in T₁ states compared with those in S₀ states (~0.068 Å). This change indicates that the interaction between metal and pic will be strengthened in T₁ states compared with the interaction between metal and (F)pmb ligands; thus, the ligand pic will have greater effect on frontier molecular orbitals (FMOs) in the excited state.

FMO properties

It is known that the observed differences in optical and chemical properties of these complexes depend mainly on the changes of the ground-state electronic structure. The concept of emission color turning by grafting various substituents and use the electron-withdrawing substituents at the cyclometalating ring relies on the fact that the lowest excited state is relatively well described as an HOMO to LUMO transition in a given ligand.^[23] Therefore, we will discuss in detail the ground-state electronic structure with the special emphasis on the HOMO and LUMO distribution, energy levels, and energy gaps. To illustrate the FOM nature of the complexes, we also listed the result of the Fircip by Yang et al.^[24] The FMO

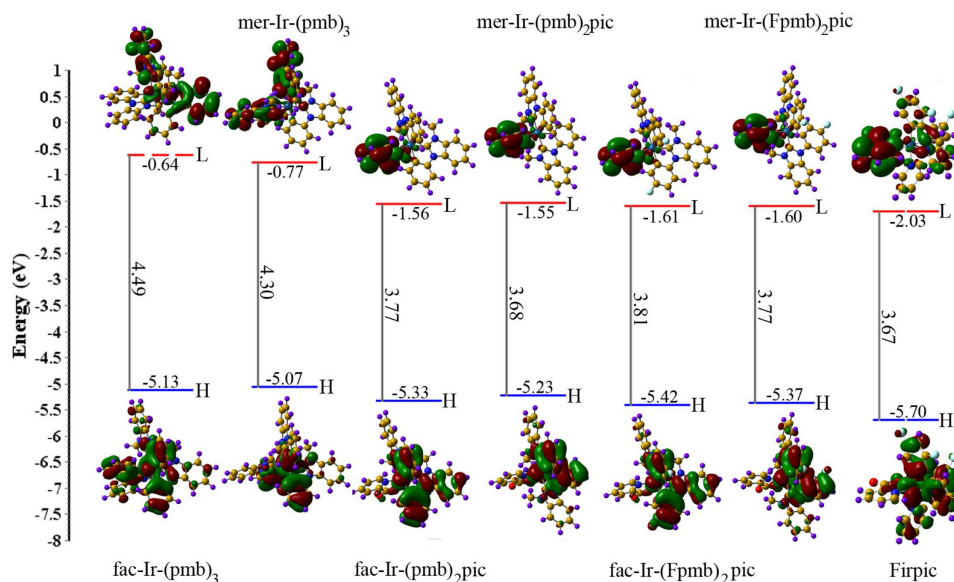


Figure 3. Presentation of the energy levels, energy gaps, and orbital composition distribution of the HOMO and the LUMO for the complexes together with Firpic.^[24] [Color figure can be viewed in the online issue, which is available at wileyonlinelibrary.com.]

compositions of the complexes 1–7 [1&2: fac- & mer-Ir-(pmb)₃; 3&4: fac- & mer-Ir-(pmb)₂pic; 5&6: fac- & mer-Ir-(Fpmb)₂pic; 7: Firpic^[24]] are given in Supporting Information Tables S1–S7. The HOMO and LUMO distribution, energy levels, and energy gaps are plotted in Figure 3.

For fac-Ir-(pmb)₃, Figure 3, Supporting Information Figure S1 and Table S1 show that the HOMO mainly resides on the metal (42%) and the phenyl moieties (19%), and the metal d orbital is an antibonding combination with the phenyl moieties π -orbital. The HOMO of mer-Ir-(pmb)₃ has a different distribution to fac-isomer, one of the three ligands nearly having no contribution to the HOMO because of the lower molecular symmetry, and the composition on the other two ligands are 24 and 26%, respectively. But, the LUMO of them are very similar. So there is a lot of energy will be radiated as the thermal radiation when the electrons jumped to the HOMO from the LUMO, maybe that is why the Ir-(pmb)₃ complexes have a low luminescence quantum yield ($\Phi = 0.04$). For Firpic, the HOMO extends over the d orbital of the Ir atom and the two Fppy ligands, which is more evenly distributed, whereas the LUMO not only extends over the pic ligand, but also distributes on a Fppy ligand a little, thus, for Firpic, it is also difficult to get to a higher luminescence quantum yield like the red and yellow light-emitting Ir(III) complexes. However, for Ir-(Rpmb)₂pic complexes, whose FMO properties are very similar, the HOMO extends over the d orbital of the Ir atom and the two Rpmb ligands π -orbital character, whereas the LUMO extends over the pic ligand π^* -orbital character. Namely, the energy of the electronic transition from LUMO to HOMO will be used for photon radiation completely, so we expect that the Ir-(Rpmb)₂pic [fac- and mer-Ir-(Rpmb)₂pic] complexes will get to a higher luminescence quantum yield compare to the Firpic complex. Details of other orbital compositions can be seen from Supporting Information Tables S1–S7.

Moreover, the energy levels of HOMO and LUMO are greatly influenced by the ancillary ligands pic. Figure 3 shows that the Ir-(pmb)₃ complexes have generally the higher HOMO and LUMO levels, but the pic group can decrease both of the HOMO (~ 0.18 eV) and LUMO (~ 0.86 eV) energy levels, and the LUMO level decreased more seriously. Namely, the pic group also decreased the H–L gap (~ 0.72 eV) for Ir-(pmb)₂pic complexes. Conversely, the electron-withdrawing group —F, which has the effect of stabilizing the HOMO level (~ 0.13 eV) while only slightly affecting the LUMO level (~ 0.05 eV), increased the H–L gap for Ir-(Fpmb)₂pic complexes. However, compare to the Firpic complex,^[24] both of the HOMO and LUMO energy levels are higher for the Ir-(Rpmb)₂pic complexes while the H–L gap is smaller. Compare to the Ir-(pmb)₃ complexes, the decreased LUMO energy levels will benefit the electron injection, whereas compare to the Firpic complex, the raised HOMO levels will increase the hole injection ability. These relative HOMO and LUMO energy levels will guide to compare the EL efficiency of OLEDs among these complexes, and this will be discussed in the next section.

Ionization potentials and OLED device

In this section, ionization potentials (IPs), reorganization energy (λ), and "small polaron" stabilization energy (SPE) are calculated for these complexes, together with hole extraction potential (HEP). The IP is used to evaluate the energy barrier for the injection of holes, and the reorganization energy is used to evaluate the charge transfer rate and balance. IP can be for either vertical excitations (v ; at the geometry of the neutral molecule) or adiabatic excitations (a ; optimized structure for both the neutral and charged molecule). HEP is the energy difference from M (neutral molecule) to M⁺ (cationic), using the M⁺ geometric structure in the calculation. SPE is used to estimate self-trapping energies of charge in the

materials, which is the energy gain of the excess charge due to a structural relaxation, that is, the difference between IP(a) and IP(v). For photoluminescent materials, a smaller IP value means easier to inject holes into the device. As Figure 3 shown, the target complexes Ir-(Rpmb)₂pic have the similar LUMO levels with Firpic complex in our work, so we would not discuss the materials characters of the electrons injection abilities for the devices in this article.

As shown in Table 2, the IP values are similar for the investigated complexes Ir-(Rpmb)₂pic, 6.01–6.28 eV for adiabatic and 6.17–6.41 eV for vertical ones, respectively, which are consistent with the HOMO energy sequence. These similar IP values indicate similar holes injection abilities. But the complexes Ir-(pmb)₃, who have the lower IP values, have the better holes injection abilities than Ir-(Rpmb)₂pic complexes.

According to the Marcus–Hush model,^[25] the charge transfer rate, *k*, can be expressed by the following formula:

$$k = \left(\frac{\pi}{\lambda k_b T} \right)^{\frac{1}{2}} \frac{V^2}{\eta} \exp \left(-\frac{\lambda}{4k_b T} \right) \quad (1)$$

where *T* is the temperature, *k_b* is the Boltzmann constant, *λ* is the reorganization energy, and *V* is the coupling matrix element between the ions and molecules which is dictated by the overlap of orbitals. As shown in Eq. (1), there are two factors, *λ* and *V*, determine *k*. Due to the limited intermolecular charge transfer range in the solid state, the mobility of charges has been demonstrated to be largely related to the reorganization energy, *λ*, for OLED materials.^[26] Generally, *λ* is determined by fast changes in molecular geometry (the internal reorganization energy, *λ_{hole}*) and by slow variations in the surrounding medium (the external reorganization energy, *λ_e*). In OLED devices, the contribution from *λ_e* can be neglected. Therefore, the internal reorganization energy *λ_{hole}* is the determining factor. The *λ_{hole}* for hole transfer can be expressed as follows:^[27]

$$\lambda_{\text{hole}} = \lambda_0 + \lambda_+ = (E_0^* - E_0) + (E_+^* - E_+) = \text{IP(v)} - \text{HEP} \quad (2)$$

as illustrated in Figure 4, *E₀* and *E₊* represent the energies of the neutral and cation species in their lowest energy geometries, respectively, whereas *E₀^{*}* and *E₊^{*}* represent the energies of the neutral and cation species with the geometries of the cation and neutral species, respectively.^[27] Emitting layer materials need to achieve hole and electron injection and transport

Energies (eV)	Ir(pmb) ₃		(pmb) ₂ Irpic		(Fpmb) ₂ Irpic	
	Facial	Meridional	Facial	Meridional	Facial	Meridional
IP (a)	5.86	5.63	6.10	6.01	6.28	6.23
IP (v)	5.92	5.91	6.25	6.17	6.41	6.38
HEP	5.78	5.32	5.90	5.84	6.14	6.07
SPE (h)	0.06	0.28	0.14	0.16	0.12	0.15
<i>λ_{hole}</i>	0.20	0.20	0.23	0.23	0.24	0.24

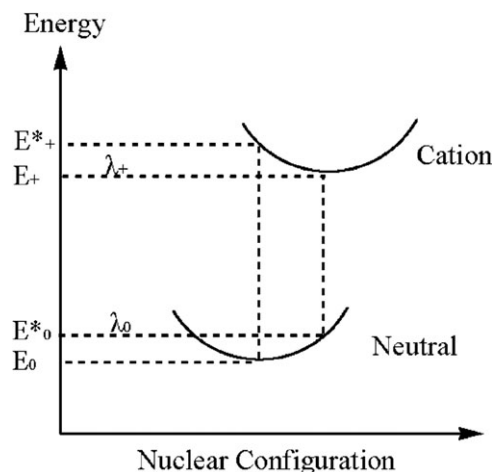


Figure 4. Schematic description of internal reorganization energy for hole transfer.

balance, and the reorganization energy has a certain influence on the charge transport process, so, the discuss of the reorganization energy is necessary in here. In our previous work, we found that for most complexes, the reorganization energies for hole transport (*λ_{hole}*) are larger than those for electron transport (*λ_{electron}*), since that the electron transport performance of these complexes is better than for hole, that is, improve the hole transport ability of the materials is essential. So in this article, the complexes Ir-(Rpmb)₂pic, who have the lower *λ_{hole}* value (0.23–0.24 eV) in comparison with the Firpic complex (0.39 eV),^[24] will have a better charge transport properties.

To compare the EL efficiency of OLED devices with these Ir (III) complexes as emission materials, the device configuration and energy levels for these complexes are shown in Figure 5. For ease of comparison, we take the absolute value of the energy. Generally, OLED devices with a three-layer structure were fabricated, the holes transition layer (HTL), the emitting layer (EML), and the electrons transition layer (ETL), together

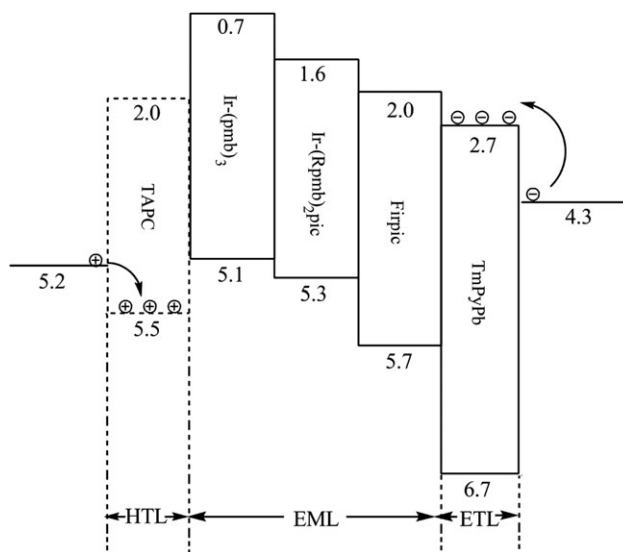


Figure 5. The device structure of the materials we designed in this work.

Table 3. Calculated absorption of the complexes in CH₂Cl₂ media at TD-B3LYP level, together with experimental values.

Complex	States	λ (nm)/E (eV)	Exptl ^[a] λ (nm)	Oscillator	Main configurations	Assign	
fac-Ir-(pmb) ₃	S1	329/3.78	270–360	0.056	HOMO→LUMO(68%)	Ir/pmb1/pmb2/pmb3→pmb2/pmb3(MLCT/LLCT/ILCT)	
	S5	301/4.12	270–360	0.108	HOMO-1→LUMO+2(59%)	Ir/pmb2/pmb3→pmb2/pmb3(MLCT/LLCT/ILCT)	
	S19	268/4.63	<270	0.086	HOMO-4→LUMO+1(32%)	pmb2/pmb3→pmb1(LLCT)	
					HOMO-4→LUMO+2(36%)	pmb2/pmb3→pmb2/pmb3(LLCT/ILCT)	
					HOMO-4→LUMO+2(48%)	pmb2/pmb3→pmb2/pmb3(LLCT/ILCT)	
					HOMO-4→LUMO+5(39%)	pmb2/pmb3→pmb1/pmb2/pmb3(LLCT/ILCT)	
	S20	267/4.63		0.086	HOMO-3→LUMO+4(37%)	pmb1→pmb2/pmb3(LLCT)	
	S50	237/5.22		0.064	HOMO-4→LUMO+4(30%)	pmb2/pmb3→pmb2/pmb3(LLCT/ILCT)	
	S51	237/5.23		0.229	HOMO-3→LUMO+5(30%)	pmb1→pmb1/pmb2/pmb3(LLCT/ILCT)	
	mer-Ir-(pmb) ₃	S1	342/3.62		0.009	HOMO→LUMO(69%)	Ir/pmb1/pmb2→pmb2/pmb3(MLCT/LLCT/ILCT)
S7		298/4.17	290–310	0.246	HOMO-2→LUMO(63%)	pmb2→pmb2/pmb3(LLCT/ILCT)	
S40		244/5.07	230–250	0.092	HOMO-7→LUMO(49%)	pmb1/pmb2/pmb3→pmb2/pmb3(LLCT/ILCT)	
S41		244/5.09		0.126	HOMO→LUMO+11(36%)	Ir/pmb1/pmb2→pmb1/pmb3(MLCT/LLCT/ILCT)	
S52		235/5.28		0.043	HOMO-4→LUMO+5(27%)	pmb1/pmb3→pmb1(LLCT/ILCT)	
S53		235/5.29		0.119	HOMO-1→LUMO+11(29%)	Ir/pmb1/pmb3→pmb1/pmb3(MLCT/LLCT/ILCT)	
					HOMO-1→LUMO+10(32%)	Ir/pmb1/pmb3→pmb1/pmb2/pmb3(MLCT/LLCT/ILCT)	
					HOMO-4→LUMO+5(30%)	pmb1/pmb3→pmb1(LLCT/ILCT)	
					HOMO→LUMO(70%)	Ir/pmb1/pmb2→pic(MLCT/LLCT)	
fac-Ir-(pmb) ₂ pic		S1	403/3.08		0.002	HOMO→LUMO(70%)	Ir/pmb1/pmb2→pmb1/pmb2(MLCT/LLCT/ILCT)
	S10	306/4.06		0.166	HOMO-1→LUMO+3(65%)	Ir/pmb1/pmb2→pmb1/pmb2(MLCT/LLCT/ILCT)	
	S28	259/4.78		0.081	HOMO-4→LUMO+3(53%)	Ir/pmb1/pmb2→pmb1/pmb2(MLCT/LLCT/ILCT)	
	S29	258/4.81		0.134	HOMO-4→LUMO+2(39%)	Ir/pmb1/pmb2→pmb1/pmb2(MLCT/LLCT/ILCT)	
	S48	238/5.21		0.09	HOMO-1→LUMO+5(32%)	Ir/pmb1/pmb2→pmb2(MLCT/LLCT/ILCT)	
					HOMO-2→LUMO+5(34%)	Ir/pmb1/pmb2→pmb2(MLCT/LLCT/ILCT)	
		S49	237/5.22		0.089	HOMO-13→LUMO(36%)	pic→pic(ILCT)
					0.001	HOMO→LUMO(70%)	Ir/pmb1/pmb2→pic(MLCT/LLCT)
	mer-Ir-(pmb) ₂ pic	S1	416/2.98		0.001	HOMO→LUMO(70%)	Ir/pmb1/pmb2→pic(MLCT/LLCT)
		S15	286/4.34		0.215	HOMO-2→LUMO+2(44%)	Ir/pmb1/pmb2→pmb1/pmb2(MLCT/LLCT/ILCT)
S34		248/4.99		0.077	HOMO-4→LUMO+3(35%)	Ir/pmb1/pmb2→pmb1/pmb2(MLCT/LLCT/ILCT)	
S35		247/5.02		0.031	HOMO-2→LUMO+4(34%)	Ir/pmb1/pmb2→pmb1/pmb2(MLCT/LLCT/ILCT)	
					HOMO-5→LUMO+2(24%)	pmb1/pmb2→pmb1/pmb2(LLCT/ILCT)	
					HOMO→LUMO+7(24%)	Ir/pmb1/pmb2→pmb1/pmb2(MLCT/LLCT/ILCT)	
					0.097	HOMO-3→LUMO+4(37%)	Ir/pmb1/pmb2/pic→pmb1/pmb2(MLCT/LLCT/ILCT)
S44		240/5.16		0.097	HOMO-3→LUMO+5(36%)	Ir/pmb1/pmb2/pic→pmb1/pmb2(MLCT/LLCT/ILCT)	
S45		238/5.21		0.142	HOMO-3→LUMO+5(36%)	Ir/pmb1/pmb2/pic→pmb1/pmb2(MLCT/LLCT/ILCT)	
fac-Ir-(Fpmb) ₂ pic		S1	395/3.14		0.002	HOMO→LUMO(70%)	Ir/Fpmb1/Fpmb2→pic(MLCT/LLCT)
	S12	301/4.12		0.102	HOMO-1→LUMO+3(57%)	Ir/Fpmb1/Fpmb2→Fpmb1/Fpmb2(MLCT/LLCT/ILCT)	
	S27	260/4.77		0.194	HOMO-4→LUMO+3(46%)	Ir/Fpmb1/Fpmb2→Fpmb1/Fpmb2(MLCT/LLCT/ILCT)	
	S29	258/4.81		0.141	HOMO-1→LUMO+6(34%)	Ir/Fpmb1/Fpmb2→Fpmb1/Fpmb2(MLCT/LLCT/ILCT)	
	S48	237/5.22		0.115	HOMO-5→LUMO+2(37%)	Ir/Fpmb1/Fpmb2/pic→Fpmb1/Fpmb2(MLCT/LLCT/ILCT)	
	S50	236/5.26		0.082	HOMO-2→LUMO+5(38%)	Ir/Fpmb1/Fpmb2→Fpmb2(MLCT/LLCT/ILCT)	
	mer-Ir-(Fpmb) ₂ pic	S1	402/3.08		0.001	HOMO→LUMO(70%)	Ir/Fpmb1/Fpmb2→pic(MLCT/LLCT)
		S14	284/4.36		0.157	HOMO-2→LUMO+2(60%)	Ir/Fpmb1/Fpmb2→Fpmb1/Fpmb2(MLCT/LLCT/ILCT)
		S32	252/4.93		0.414	HOMO-1→LUMO+5(56%)	Ir/Fpmb1/Fpmb2→Fpmb1/Fpmb2(MLCT/LLCT/ILCT)
		S33	250/4.95		0.02	HOMO-8→LUMO(41%)	Fpmb1/Fpmb2→pic(LLCT)
S48		235/5.29		0.057	HOMO-3→LUMO+6(31%)	Ir/Fpmb1/Fpmb2/pic→Fpmb1/Fpmb2(MLCT/LLCT/ILCT)	
S50		233/5.32		0.128	HOMO-3→LUMO+5(33%)	Ir/Fpmb1/Fpmb2/pic→Fpmb1/Fpmb2(MLCT/LLCT/ILCT)	
Firpic ^[b]		425		0.008	HOMO→LUMO(96%)	MLCT/LLCT	

[a] Ref. [6]. [b] Ref. [24].

with the indium tin oxide (ITO), whose work function is 5.2 eV, as anode and lithium fluoride (LiF)/aluminum (Al) (LiF/Al) as cathode. The materials TAPC (di-[4-(N,N-ditoly-amino)-phenyl]-cyclohexane) and TmPyPb (1,3,5-tri[m-pyrid-3-yl-phenyl] benzene) are used as the charge transporting layer (HTL and ETL, respectively) nowadays,^[28] since their suitable HOMO and LUMO energy levels for Ir (III) complexes.

For Ir-(pmb)₃ complexes, the HOMO level (~5.1 eV) is similar to the work function of ITO, what will be fit for the holes transition directly, but the TAPC has a lower HOMO level (5.5 eV), so the HTL is reactive in here, that is, the HTL of the device for Ir-(pmb)₃ complexes is needless. However, for the LUMO levels, the Ir-(pmb)₃ (~0.7 eV) is higher than TmPyPb (~2.7 eV) 2.0 eV, it is very difficult to inject for electrons, maybe this is a

reason of the Ir-(pmb)₃ complexes have a lower luminescence quantum yield (~0.04). For Firpic complex, the HOMO energy level (5.7 eV) is lower than ITO 0.5 eV, so that, it is necessary for HTL (TAPC) in here, and the barrier of the electrons injection is 0.7 eV, which is easier for electrons to be injected in the EML; thus, the Firpic complex has a higher luminescence quantum yield (~0.10). And for the Ir-(Rpmb)₂pic complexes, the LUMO level located between Ir-(pmb)₃ and Firpic, which means that the electrons injection will be easier than Ir-(pmb)₃ but a little harder than Firpic, conversely, the HOMO level of them are very similar to the work function of ITO, that means the HTL (TAPC) also can be omitted in the devices, and then, the devices will be simpler and the transmittance will be enhanced.

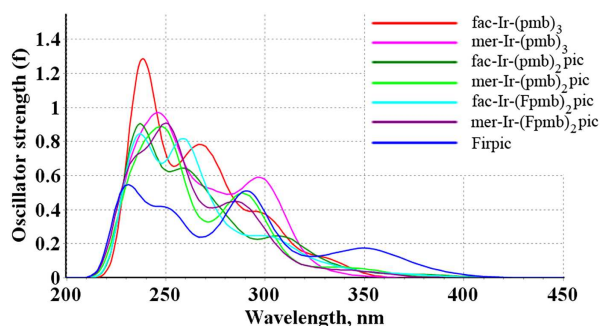


Figure 6. Simulated absorption spectra of the complexes in CH_2Cl_2 media with the calculated data under the TD-B3LYP/LANL2DZ level together with Firpic.^[24] [Color figure can be viewed in the online issue, which is available at wileyonlinelibrary.com.]

Absorption in CH_2Cl_2 media

The calculated absorption spectra associated with their oscillator strengths, assignment, and excitation energies are listed in Table 3, the FMO properties are listed in Supporting Information Table S1–S7. For clarity, only the leading excited states (with larger CI coefficients) are listed. The calculated lowest-lying absorption of Ir-(pmb)₃ complexes are comparable to the experimental value.^[6] The fitted Gaussian type absorption curve is depicted in Figure 6. We also calculated the HOMO and LUMO energy levels of Ir-(pmb)₃ complexes by 6-31+G(d,p) basis set, shown in Supporting Information Figure S4, and the result shown that there is no much more difference between basis set 6-31+G(d,p) and 6-31G*. So in final, to save the time of computing, all the complexes were calculated by 6-31G*.

As shown in Table 3, the lowest absorption bands of the complexes are 329, 342, 403, 416, 395, and 402 nm, respectively, and the HOMO–LUMOs (~70%) are the predominant transition. Ir-(Rpmb)₂pic complexes have red shift on absorption compared with complexes Ir-(pmb)₃ but blue shift by comparing with Firpic (see Figure 6),^[24] this is due to the ligand fragments, the LUMO orbitals are located on the pic ligand and the HOMO orbitals are located on main ligands (Rpmb) for Ir-(Rpmb)₂pic complexes, so the LUMO decreased comparing to Ir-(pmb)₃ complexes and the HOMO level increased comparing to Firpic. The absorption of Ir-(pmb)₃ can be assigned to a $[d(\text{Ir})/\pi(\text{pmb}1+\text{pmb}2+\text{pmb}3)\rightarrow\pi^*(\text{pmb}2+\text{pmb}3)]$ transition with MLCT, ligand-to-ligand charge transfer (LLCT), and interligand charge transfer (ILCT) transition characters, whereas for

Ir-(Rpmb)₂pic, it can be assigned to MLCT and LLCT transition characters as summarized in Table 3.

Remarkably, all the important transitions with the greatest oscillation strengths are not attributed by HOMO–LUMO transition. By taking fac-Ir-(pmb)₂pic, for example, the absorption at 306 nm with the highest oscillation strength is attributed to HOMO-1→LUMO+3 (65%). The HOMO-1 is mostly localized on the pmb ligands and Ir atom, and the pmb ligands are predominantly responsible for the distribution of LUMO+3, the excitation HOMO-1→LUMO+3 can be assigned to $[d(\text{Ir})/\pi(\text{pmb}1+\text{pmb}2)]\rightarrow\pi^*(\text{pmb}1+\text{pmb}2)]$ transition with the MLCT, ILCT, and slightly LLCT transition characters. In the same way, all the intense absorption bands of the other complexes have been summarized in Table 3.

Emission in THF media

On the basis of the triplet excited-state geometries, we obtained the emission spectra of the six complexes at the TDDFT/M062X/LanL2DZ;6-31G* level of theory within THF solution provided by PCM, and the results are listed in Table 4, associated with the emissive energies, assignments, and the experimental values.

The calculated emission of fac- and mer-Ir-(pmb)₃ at 396.01 and 433.76 nm are comparable to the experimental value, 389–405 and 415 nm in THF media,^[29] respectively, and the Firpic calculated results with the same method to us by Yang et al. were convincingly, so we consider that the emission result calculated by us for Ir-(Rpmb)₂pic complexes are credible.

For fac-isomers, the emission peaks are red-shifted from 396 nm in Ir-(pmb)₃ to 468 and 460 nm in Ir-(pmb)₂pic and Ir-(Fpmb)₂pic, respectively; whereas for mer-isomers, the emission peaks are blue-shifted from 433 nm in Ir-(pmb)₃ to 411 and 408 nm in Ir-(pmb)₂pic and Ir-(Fpmb)₂pic. This is because that the three ligands in mer-Ir-(pmb)₃ are not equivalently, and the pic ligand masters the LUMO of mer-Ir-(Rpmb)₂pic complexes, so that, the emissions are blue-shifted from mer-Ir-(pmb)₃ to mer-Ir-(Rpmb)₂pic complexes but it is opposite for fac-isomers, except that, our result proved that the electron-withdrawing fluoride can cause a blue-shift on the emission spectra of Ir(III) complexes again.^[30] According to our calculation, as Table S1 (Supporting information) shown, the LUMO of fac-Ir-(pmb)₃ is delocalized on pmb2 and pmb3 ligand with 30% and 59% contribution, respectively, whereas the HOMO is delocalized on Ir metal (42%) and the three pmb ligands (19%). Therefore, the

Table 4. Phosphorescent emissions of the THF solution under the TD-M062X calculations, together with the experimental values and the Firpic complex.

Complex	Emissions (nm/eV)	Exptl (nm) ^[a]	Major contribution	Character
fac-Ir-(pmb) ₃	396.01/3.1309	389–405	L→H(60%)	³ MLCT/ ³ LLCT/ ³ ILCT
mer-Ir-(pmb) ₃	433.76/2.8584	415	L→H(64%)	³ MLCT/ ³ LLCT/ ³ ILCT
fac-Ir-(pmb) ₂ pic	467.79/2.6504		L→H(58%)	³ MLCT/ ³ LLCT
mer-Ir-(pmb) ₂ pic	411.24/3.0149		L→H(60%)	³ MLCT/ ³ LLCT
fac-Ir-(Fpmb) ₂ pic	459.92/2.6958		L→H(54%)	³ MLCT/ ³ LLCT
mer-Ir-(Fpmb) ₂ pic	407.53/3.0424		L→H(54%)	³ MLCT/ ³ LLCT
Firpic ^[b]	496.73		L→H(31%); L+1→H(21%)	³ MLCT/ ³ LLCT

[a] Ref. [29]. [b] Ref. [24].


observed emission can be assigned as ³ILCT transition within pmb2 and pmb3 ligands, respectively, and ³LLCT transitions as $\pi^*(\text{pmb}2) \rightarrow \pi^*(\text{pmb}1)$ and $\pi^*(\text{pmb}3) \rightarrow \pi^*(\text{pmb}1)$, and mixed with little contribution of ligand-to-metal charge transfer (³LMCT) transition from π^* orbital of pmb2 and pmb3 ligands to d orbital of Ir metal. In the same way, the FMO compositions responsible for the emissions and the transition characters of the other complexes have also been analyzed. The relative information has been listed in Table 4 and the FMO properties listed in Supporting Information Tables S1–S7.

Conclusion

To find a pure-blue lighting-emission with high luminescence quantum yield material of iridium(III) cyclometalated complexes, we have carried out DFT/B3LYP and TDDFT/B3LYP calculations on the geometrical structures, absorptions, injection, and transport abilities, phosphorescence mechanism (TDDFT/M062X) with the LANL2DZ basis set was used on metal atom Ir and the 6-31G* basis set on C, H, N, O, and F atoms in all the calculations. The calculated results of the Ir-(pmb)₃ complexes are comparable to the experimental. The calculation reveals that the changes of the auxiliary ligand and the use of the electron-withdrawing substituents can effectively influence the HOMO–LUMO gap and the emission color. Furthermore, the Ir-(pmb)₂pic complexes designed in this article have the true blue color of the light-emitting (408–468 nm), and they have the similar HOMO with Ir-(pmb)₃ and the similar LUMO with the Firpic, this means that the charges injection will be very easy. In addition, the HOMO energy levels of the Ir-(pmb)₂pic complexes are lower than work function of the ITO (the anode of the OLEDs) 0.1 eV, this means that the light-emitting materials can be deposited on ITO surface directly, namely, the OLED device of the Ir-(pmb)₂pic complexes will have a high transmittance. We hope these theoretical studies can provide some help in designing highly efficient phosphorescent materials of the experiment.

Keywords: organic light-emitting displays · Ir(III) complex-time-dependent density-functional theory · excited state · electroluminescence

How to cite this article: M.-X. Song, Z.-M. Hao, Z.-J. Wu, S.-Y. Song, L. Zhou, R.-P. Deng, H.-J. Zhang, *Int. J. Quantum Chem.* **2013**, *113*, 1641–1649. DOI: 10.1002/qua.24379

 Additional Supporting Information may be found in the online version of this article.

- [1] (a) M. S. Lowry, S. Bernhard, *Chem. Eur. J.* **2006**, *12*, 7970; (b) K. K.-W. Lo, W.-K. Hui, C.-K. Cheng, K. H.-K. Tsang, D. C.-M. Ng, N. Zhu, K.-K. Cheung, *Coord. Chem. Rev.* **2005**, *249*, 1434; (c) Z. H. Kakafi, *Organic Electroluminescence*; CRC Press: New York, **2005**; (d) K. Müllen, U. Scherf, *Organic Light-Emitting Devices*; Wiley-VCH: Weinheim, Germany, **2006**; (e) Z. Li, H. Meng, *Organic Light-Emitting Materials and Devices*; CRC Press: Boca Raton, FL, **2006**; (f) H. Yersin, Ed. *Highly Efficient OLEDs with Phosphorescent Materials*; Wiley-VCH: Weinheim, Germany, **2008**.
- [2] K. T. Kamtekar, A. P. Monkman, M. R. Bryce, *Adv. Mater.* **2010**, *22*, 572.
- [3] (a) E. Holder, B. M. W. Langeveld, U. S. Schubert, *Adv. Mater.* **2005**, *17*, 1109; (b) P.-T. Chou, Y. Chi, *Chem. Eur. J.* **2007**, *13*, 380; (c) W.-Y. Wong, C.-L. Ho, *J. Mater. Chem.* **2009**, *19*, 4457.
- [4] (a) C. Adachi, M. A. Baldo, S. R. Forrest, M. E. Thompson, *Appl. Phys. Lett.* **2000**, *77*, 904; (b) F. Hua, S. Kinayyigit, J. R. Cable, F. N. Castellano, *Inorg. Chem.* **2005**, *44*, 471; (c) J. Kavitha, S. Y. Chang, Y. Chi, J. K. Yu, Y. H. Hu, P. T. Chou, S. M. Peng, G. H. Lee, Y. T. Tao, C. H. Chien, A. J. Carty, *Adv. Funct. Mater.* **2005**, *15*, 223; (d) T. D. Anthopoulos, M. J. Frampton, E. B. Namdas, P. L. Burn, I. D. W. Samuel, *Adv. Mater.* **2004**, *16*, 557.
- [5] (a) D. J. Stufkens, A. Vlcek, *Jr. Coord. Chem. Rev.* **1998**, *177*, 127; (b) S. Ranjan, S. Y. Lin, K. C. Hwang, Y. Chi, W. L. Ching, C. S. Liu, *Inorg. Chem.* **2003**, *42*, 1248.
- [6] (a) T. Sajoto, P. I. Djurovich, A. Tamayo, M. Yousufuddin, R. Bau, M. E. Thompson, R. J. Holmes, S. R. Forrest, *Inorg. Chem.* **2005**, *44*, 7992; (b) M. M. Begona, B. David, H. Egelhaaf, G. Johannes, *J. Chem. Phys.* **2007**, *126*, 111101.
- [7] (a) A. B. Tamayo, B. D. Alleyne, P. I. Djurovich, S. Lamansky, I. Tsyba, N. N. Ho, R. Bau, M. E. Thompson, *J. Am. Chem. Soc.* **2003**, *125*, 7377; (b) V. V. Grushin, N. Herron, D. D. LeCloux, W. J. Marshall, V. A. Petrov, Y. Wang, *Chem. Commun.* **2001**, *16*, 1494; (c) R. Ragni, E. A. Plummer, K. Brunner, J. W. Hofstraat, F. Babudri, G. M. Farinola, F. Naso, Cola. L. DeJ. *Mater. Chem.* **2006**, *16*, 1161.
- [8] J. Li, P. I. Djurovich, B. D. Alleyne, M. Yousufuddin, N. N. Ho, J. C. Thomas, J. C. Peters, R. Bau, M. E. Thompson, *Inorg. Chem.* **2005**, *44*, 1713.
- [9] (a) T. Sajoto, P. I. Djurovich, A. Tamayo, M. Yousufuddin, R. Bau, M. E. Thompson, R. J. Holmes, S. R. Forrest, *Inorg. Chem.* **2005**, *44*, 7992; (b) K. Dedeian, J. M. Shi, N. Shepherd, E. Forsythe, D. C. Morton, *Inorg. Chem.* **2005**, *44*, 4445; (c) P. Coppo, E. A. Plummer, Cola. L. De *Chem. Commun.* **2004**, 1774; (d) E. J. Nam, J. H. Kim, B. O. Kim, S. M. Kim, N. G. Park, Y. S. Kim, Y. K. Kim, Y. Ha, *Bull. Chem. Soc. Jpn.* **2004**, *77*, 751; (e) C. H. Yang, S. W. Li, Y. Chi, Y. M. Cheng, Y. S. Yeh, P. T. Chou, G. H. Lee, C. H. Wang, C. F. Shu, *Inorg. Chem.* **2005**, *44*, 7770; (f) C. S. K. Mak, A. Hayer, S. I. Pascu, S. E. Watkins, A. B. Holmes, A. Kohler, R. H. Friend, *Chem. Commun.* **2005**, *37*, 4708; (g) S.-C. Lo, *Chem. Mater.* **2006**, *18*, 5159.
- [10] W. J. Finkenzeller, H. Yersin, *Chem. Phys. Lett.* **2003**, *377*, 299.
- [11] Y. Kawamura, K. Goushi, J. Brooks, J. J. Brown, H. Sasabe, C. Adachi, *Appl. Phys. Lett.* **2005**, *86*, 71104.
- [12] F. C. Wu, R. B. Mills, R. D. Evans, P. J. Dillon, *Anal. Chem.* **2004**, *76*, 110.
- [13] (a) R. Terki, L. P. Simoneau, A. Rochefort, *J. Phys. Chem. A.* **2009**, *113*, 534; (b) T. Liu, B. H. Xia, X. Zhou, Q. C. Zheng, Q. J. Pan, H. X. Zhang, *Theor. Chem. Acc.* **2008**, *121*, 155.
- [14] M. J. Frisch, Gaussian 09, Revision A.02; Gaussian Inc.: Wallingford, CT, **2009**.
- [15] E. Runge, E. K. U. Gross, *Phys. Rev. Lett.* **1984**, *52*, 997.
- [16] M. Petersilka, U. J. Gossmann, E. K. U. Gross, *Phys. Rev. Lett.* **1996**, *76*, 1212.
- [17] S. L. Mayo, B. D. Olafson, W. A. Goddard, III, *J. Phys. Chem.* **1990**, *94*, 8897.
- [18] B. Mennucci, J. Tomasi, *J. Chem. Phys.* **1997**, *106*, 5151.
- [19] (a) X. Li, X. Liu, Z. Wu, H. Zhang, *J. Phys. Chem. A.* **2008**, *112*, 11190; (b) X. Li, Z. Wu, H. Zhang, Z. Si, L. Zhou, X. Liu, *Eur. J. Inorg. Chem.* **2009**, *27*, 4052; (c) X. Li, Z. Wu, Z. Si, H. Zhang, L. Zhou, X. Liu, *Inorg. Chem.* **2009**, *48*, 7740; (d) X. Li, Z. Wu, H. Zhang, X. Liu, L. Zhou, Z. Li, Z. Si, *Phys. Chem. Chem. Phys.* **2009**, *11*, 6051.
- [20] Y. Zhao, D. G. Truhlar, *J. Phys. Chem. A.* **2006**, *110*, 5121.
- [21] P. J. Hay, W. R. Wadt, *J. Chem. Phys.* **1985**, *82*, 299.
- [22] (a) L. Shi, B. Hong, W. Guan, Z. Wu, Z. Su, *J. Phys. Chem. A.* **2010**, *114*, 6559; (b) D. Nie, Z. Liu, Z. Bian, C. Huang, *J. Mol. Struct.: Theochem.* **2008**, *861*, 97.
- [23] I. Avilov, P. Minoofar, J. Cornil, L. De Cola, *J. Am. Chem. Soc.* **2007**, *129*, 8247.
- [24] B. Yang, M. Zhang, H. Zhang, J. Sun, *J. Lumin.* **2011**, *131*, 1158.
- [25] (a) N. S. Hush, *J. Chem. Phys.* **1958**, *28*, 962; (b) R. A. Marcus, *Rev. Mod. Phys.* **1993**, *65*, 599; (c) R. A. Marcus, *J. Chem. Phys.* **1956**, *24*, 966.

- [26] (a) M. Malagoli, J. L. Brédas, *Chem. Phys. Lett.* **2000**, 327, 13; (b) B. C. Lin, C. P. Cheng, Z. P. M. Lao, *J. Phys. Chem. A.* **2003**, 107, 5241.
- [27] G. R. Hutchison, M. A. Ratner, T. J. Marks, *J. Am. Chem. Soc.* **2005**, 127, 2339.
- [28] (a) Y. Zhu, L. Zhou, H. Li, Q. Xu, M. Teng, Y. Zheng, J. Zuo, H. Zhang, X. You, *Adv. Mater.* **2011**, 23, 4041; (b) Y. Chen, J. Chen, Y. Zhao, D. Ma, *Appl. Phys. Lett.* **2012**, 100, 213301.
- [29] R. J. Holmes, S. R. Forrest, T. Sajoto, A. Tamayo, P. I. Djurovich, M. E. Thompson, J. Brooks, Y.-J. Tung, B. W. D'Andrade, M. S. Weaver, R. C. Kwong, J. Brown, *Appl. Phys. Lett.* **2005**, 87, 243507.
- [30] L. Flamigni, A. Barbieri, C. Sabatini, B. Ventura, F. Barigelletti, *Top. Curr. Chem.* **2007**, 281, 143.

Received: 21 August 2012
 Revised: 14 November 2012
 Accepted: 3 December 2012
 Published online on 8 January 2013